Through the wall Target Detection/Monitoring from Compressively Sensed Signals via Structural Sparsity

Mehmet Yamaç[1], Melek Orhan[2,3], Bulent Sankur[4], Ahmet Serdar Turk[5], and Moncef Gabbouj[1]

[1]Tampere University of Technology, Laboratory of Signal Processing, Tampere, Finland
[4]Boğaziçi University, Electrical and Electronics Engineering Department, Istanbul, Turkey
[2]Gebze Technical University, Institute of Defense Technologies, Kocaeli, Turkey
[3]Gebze Technical University, Electronics Engineering Department, Kocaeli, Turkey
[5]Yildiz Technical University, Electronics and Communications Engineering Department, Istanbul, Turkey

***Abstract*—We develop a through-the-wall radar imaging (TWRI) system using stepped-frequency radar for the detection of stationary objects at close distances. This system uses the random frequency sampling and a structural sparsity based reconstruction method. The proposed reconstruction algorithm employs the block sparse structure and smoothness characteristics of the illuminated scene. In experiments on real data, we show that the proposed sparsity-based reconstruction algorithm outperforms the conventional ℓ_1 minimization-based radar imaging results.**

***Index Terms*—Compressive Sensing, Radar Imaging, Structural Sparsity, Random Frequency Radar Imaging**

I. Introduction

A stepped-frequency system (SFS) [1] works based on transmission of short electromagnetic waveforms at sequenced frequency steps, and measurement of the magnitude of the reflected signal and its phase difference with reference to the transmitted signal. One can consider the SFS method as a sampling in the frequency domain over a wide bandwidth. Modulated short pulses at stepped frequencies achieve ultra-bandwidth illumination of the medium, which is a crucial requirement where both low and high frequencies need to be employed as in the case of ground penetrating radar (GPR) [2] or TWRI. Other advantages of SFS list as lower transmission power, higher SNR value since the receiver is exposed to less noise in the smaller bands at stepped discrete frequencies [3], and finally use of existing efficient hardware implementation. Despite these advantages, one shortcoming is that they suffer from high data acquisition time since the radar transmitter and receiver has to operate at only a-single-frequency at-a-time. There have been some studies [4] where multi-frequencies are transmitted concurrently. However, the state-of-the-art approach is to transmit a subset of stepped frequencies and reconstruct the signal using techniques from Compressive Sensing theory [5]. In this study, we adopt this approach and use measurements of random subsets of Fourier coefficients to reconstruct the A-scan data.

There has been a recent interest in the literature in random frequency radar imaging [5], [6], [9], [10]. These works assume either a point-like sparse scene where the number of targets is less than the number of grid points in a 2-D uniformly discretized space and that the target's body is small or the whole vectorized 2-D radar image is sparse in some domain, but the sparsity is not structured. In [5], random frequency GPR measurements are considered that compressively sense the A-scan of a sparse scene and the 1-D A-scan vectors are then estimated using CS reconstruction methods. In [6], the same methodology is applied for through-the-wall imaging, but sparse estimation of A-scan vectors are further improved by applying delay-and-sum beam-forming. In [7], [8], CS is also applied in TWRI, but the authors also assume point-like sparse scene. In a different vein, [9] assumes that the scene is not necessarily sparse in the canonical base, but sparse in a specific dictionary, e.g., GPR dictionary. A SAR version of these works takes place in [10], where the authors consider the sensed 2D scene image and reconstruct the SAR image by vectorizing it and assuming sparsity in a suitable 2-D sparsifying transform included canonical domain.

These schemes, however, are not convenient for scenarios where the illuminated scene exhibits structural sparsity pattern: a block-sparse model in x-position axis where each sparse A-Scan vector shares the same support or at least these successive scan vectors encounter smooth changes. While in [5], [6], [9] each A-scan 1-D vector is reconstructed as a sparse vector and then the B-Scan 2-D radar image is constructed by concatenating them, we use a different approach and estimate consecutive A-scan vectors in ensembles over sliding intervals. We assume that in TWRI scenarios, depth data does not contain step changes unless a new object starts being seen by the A-scan. We can thus assume that each A-scan vector to be sparse and that the locations of their non-zero amplitude coefficients remain practically the same during the viewing of an object. Our approach also enables to adaptively change the measurement matrix while compressively sensing A-scan signals in every successive position if we apply the reconstruction algorithm in an on-line manner during sensing. This is because we reconstruct the 2-D scene in sliding window

mode and we can detect the energy increase in measurement if a new object comes to picture. In addition to the random frequency-based CS radar imaging, a time-domain CS radar system is also possible [11], and our algorithm would still be applicable provided the structural sparsity assumption is satisfied. The time-domain scheme, however, requires more complex hardware design and is out of the scope of this work.

We organize the rest of this paper as follows. Section II provides the notation, the mathematical preliminaries and brief review of CS theory. Section III provides a brief review of stepped-frequency radar data acquisition method and explains the compressive stepped frequency data sampling. In Section IV, we propose our ADMM based radar image reconstruction approach. Finally, experimental setup and reconstructed radar images are given and the conclusion is drawn. In this work, we set up a UWB SF-GPR scenario in the laboratory and use Anritsu Network analyzer obtain real data through the wall.

II. Preliminaries

To introduce our notation, we define, the ℓ_p norm of a vector $x \in \mathbb{R}^N$ as $\|x\|_p = \left(\sum_{i=1}^{N} |x_i|^p\right)^{1/p}$ for $p \geq 1$. For compressive sensing (CS) [12], we have m of measurements $y \in \mathbb{R}^m$ of a signal vector $S \in \mathbb{R}^N$, i.e., $y = \Psi S$ where Ψ is the $m \times N$ measurement matrix. Assuming that this signal is k-sparse in a sparsifying basis Φ, then the general compressive sensing setup becomes $y = \Psi\Phi x = Ax$, where $A = \Psi\Phi$. The compressively sampled sparse signal can be reconstructed by solving the following ℓ_1 minimization problem;

$$\min_x \ \|x\|_1 \ \text{subject to } Ax = y. \tag{1}$$

For the measurement matrix Φ one may use randomly selected m rows of an orthonormal basis, Θ, which are indexed with $\Omega \in \{1, 2, 3, ..., N\}$. With such a measurement matrix Φ, then the k-sparse signal can be exactly reconstructed as solution of (1) (see [13] for Mutual Coherence).

Finally, we define the proximal operator of a function f at a point $z \in \mathbb{R}^N$ with a parameter $\gamma > 0$ as

$$\text{prox}_{\gamma f}(z) = \arg\min_u \{f(u) + \frac{1}{2\gamma}\|u - z\|_2^2\}. \tag{2}$$

to be used in Eqs. (11) and (12).

III. Compressive GPR system

A. Stepped Frequency

Assume that the frequency of n^{th} pulse is given as,

$$f_n = f_0 + n\Delta f, \quad n = 0, ..., N-1 \tag{3}$$

where Δ_f is frequency interval. The reflected signal is defined as [14]

$$r(n,t) \approx \kappa.s(\frac{t - 2R/c}{T_d})e^{\left(-j\frac{4\pi(f_0+n\Delta f)R}{c}\right)} \tag{4}$$

where κ is a constant representing attenuation effect, c is the speed of light, $s(t)$ is the base modulated signal transmitted, R is the range and T_d is the pulse duration. Since the phase

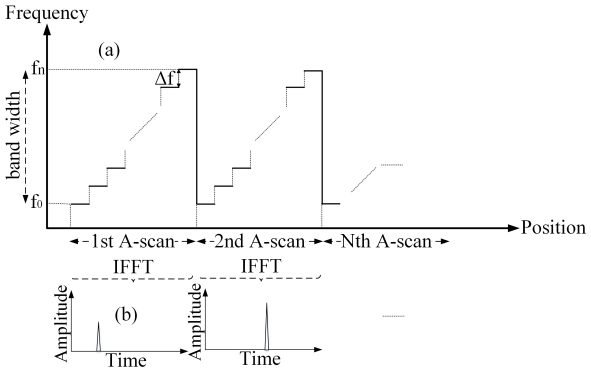

Fig. 1: Representation of stepped frequency waveform (a) transmitted signal (b) received signal after inverse Fourier transform.

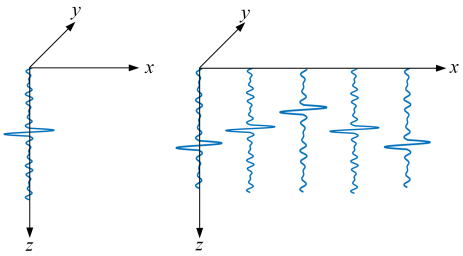

Fig. 2: Scan type of the GPR (a) A-scan (b) B-scan.

of the reflected signal is linearly related to n for a fixed R, we expect a pulse-like response in the dispersion-free case [10]. The location of this return pulse in time domain gives the depth information of the object as pictured in Figure 1.

For TWRI, we consider two scan types, the A-scan and the B-scan. The A-scan data gives the range profile corresponding to a single pulse of the radar. The radar signal sent by the transmitting antenna is reflected from the targets and the return signals are captured by the receiving antenna. The information about the target is obtained by interpreting the amplitude and phase value of the received signal.

Along the x-axis scan direction, the A-scan data is collected in constant spatial displacements to generate a 2-D matrix. This 2-D matrix allows us to create a 2-D image, called the B-scan, of the scene. This B-scan pictures the x-z reflectivity plane of the space behind the wall, where the range (z-axis) indicates the distance from the target, and the position (x-axis) defines the horizontal motion of the antenna. The method of obtaining A-Scan and B-Scan is pictured in Figure 2. It is possible to obtain a 3D image, called C-scan, including the vertical position (y-axis).

B. Incoherent Measurements

A natural selection of measurement matrix for the stepped frequency TWRI case consists in randomly choosing rows from Fourier basis F_Ω. This corresponds simply to measuring randomly m frequency responses at some location l,i.e.,

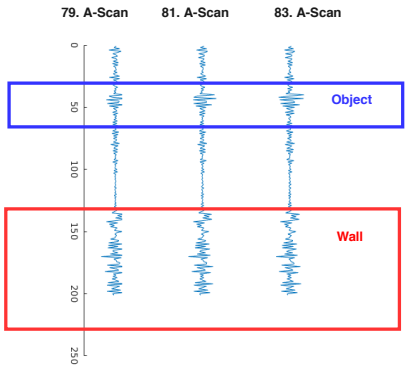

Fig. 3: A-Scan signals are obtained by taking IFFT of $N = 201$ uniformly sampled frequencies between 0.1 GHz-15 GHz at positions 79, 81 and 83.

$y_l = F_{\Omega_l} x_l$, $x \in \mathbb{R}^N$, $y \in \mathbb{R}^m$. For B-scan, one slides the TWRI device from position l to $l+1$ to take the next m measurements, $y_{l+1} = F_{\Omega_{l+1}} x_{l+1}$ and so on along the x trajectory. In this setup, each 1-D vector, x_l representing the depth information is considered to be sparse, hence amenable to CS-based reconstruction from (1).

In the ideal case where x_l is exactly k-sparse, we know that it can be exactly reconstructed if we have $m \geq O(k.logN)$ [13]. But in reality, we obtain noisy time domain A-Scans with spiky peaks in the range of object positions as illustrated in Figure 3. These signals are therefore not exactly sparse, but compressible in the sense that one may zero-out the small coefficients to make the object visible and obtain sparse range-profile.

IV. Proposed Reconstruction

Through-the-wall imaging is a well-established technique to detect and identify objects behind opaque structures. A case in point is an urgent rescue operation after an earthquake where bodies and limbs need to be identified or a terrorist attack where persons and possibly arms need to be detected behind concrete walls.

In these cases, radar imaging of a human body cannot be assumed as a point-like sparse signal. One then expects the entries in the x-z matrix of the B-scan to possess a block-sparse structure of some size D. In the B-scan matrix, l refer to each scan position of the radar as a column. Thus if there is a reflecting object behind the wall, then the B-scan non-zero coefficients will start emerging at some position l and continue the position $l+D$. Conversely, we do not expect a change vis-a-vis the background until a new object comes into picture at some location l for the duration of D A-scan steps. The non-zero coefficients from position x_l till the end of the reflecting body will continue without much variation both in (i) magnitude and (ii) indices of non-zero coefficients. Condition (i) can be satisfied by adding a total variation term to be minimized i.e., $\sum_{l=\tau}^{T+\tau-1} \|x_{l+1} - x_l\|_1$, where T is sliding window length and τ is the current position. Assumption (ii) can be satisfied if we allow the supports of non-zero coefficients in successive A-scans by minimizing the number of non-zero rows in the current window, i.e., $\sum_{i=1}^{N} \left\| x^i_{\tau:(\tau+T-1)} \right\|_2$. The necessity of this term enforcing row sparsity can be seen in Figure 3 since the non-sparse supports of successive A-Scans are expected to remain same during object. However, this row sparsifying may cause an undesirable noise effect in the solution of the system when $T >> D$. Because the non-sparse support in the solution continue to remain same for a while, i.e, between 1 to T new scan. Therefore, we may wish to divide this T A-Scan solutions into group of adjacent columns of length L with $L \leq T$. These groups can be formed in non-overlapping manner, i.e, $\underline{x}^{i,k} = x^i_{\tau+(k-1)L:(\tau+kL-1)}$, or over-lapping manner, i.e., $\underline{x}^{i,k} = x^i_{\tau+(k-1):(\tau+L+k-1)}$, where $\underline{x}^{i,k}$ is the k.th group of i.th row. We can formulate a cost function that satisfies these assumptions as follows:

$$\hat{x}_{\tau:(\tau+T)} = \arg \min_{x_{\tau:(\tau+T)}} \Big(\frac{\lambda_1}{2} \sum_{t=\tau}^{T+\tau} \|y_l - F_t x_l\|_2^2 + \lambda_2 \sum_{i=1}^{N} \sum_{k} \left\| \underline{x}^{i,k} \right\|_2 + \lambda_3 \sum_{t=\tau}^{T+\tau-1} \|x_{t+1} - x_t\|_1 \Big) \quad (5)$$

where $\lambda_1, \lambda_2, \lambda_3$ are regularization parameters. The first term is simply the data fidelity term, the second is the block sparsity constraint and the third one constrains the reflection coefficients from the object to remain the same. If we represent the concatenation of desired signals from time τ to $T+\tau$ in matrix form, i.e., $x_{\tau:(\tau+T-1)} = X \in \mathbb{R}^{N \times T}$ then we can rewrite equation (5) as

$$\hat{X} = \arg \min_X \Big(\frac{\lambda_1}{2} \sum_{d=1}^{T} \|y_d - F_d x_d\|_2^2 + \lambda_2 \|X\|_{2,1;L} + \lambda_3 \|X\|_{Tv,1} \Big) \quad (6)$$

where $\|X\|_{2,1;L} = \sum_{i=1}^{N} \sum_k \left\| \underline{x}^{i,k} \right\|_2$ parameter enforcing row base group sparsity with window length L , $X \in \mathbb{R}^{N \times T}$ is current sliding window matrix and x_d is d.th column of this matrix with corresponding measurement matrix F_d.

We will follow a ADMM based scheme to solve this problem. A consensus form of (5) can be written as

$$\left(\hat{X}, \hat{Z}_1, \hat{Z}_2 \right) = \arg \min_X \Big(\frac{\lambda_1}{2} \sum_{d=1}^{T} \|y_d - F_d x_d\|_2^2 + \lambda_2 \|Z_1\|_{2,1;L} + \lambda_3 \|Z_2\|_{Tv,1} \Big) \quad \text{subject to} \quad Z_1 = X, Z_2 = X. \quad (7)$$

The augmented Lagrangian form of (7) can be cast as

$$L(\beta_1, \beta_2, X, Z_1, Z_2) = \Big(\frac{\lambda_1}{2} \sum_{d=1}^{T} \|y_d - F_d x_d\|_2^2 + \lambda_2 \|Z_1\|_{2,1} + \lambda_3 \|Z_2\|_{Tv,1} + \langle \beta_1, (Z_1 - X) \rangle + \langle \beta_2, (Z_2 - X) \rangle + \frac{\mu_1}{2} \|X - Z_1\|_F^2 + \frac{\mu_2}{2} \|X - Z_2\|_F^2 \Big), \quad (8)$$

where the last two penalty terms with $\mu_1, \mu_2 > 0$ and $\beta_1 \in \mathbb{R}^{N \times T}, \beta_2 \in \mathbb{R}^{N \times T}$ are dual variables. In ADMM, primal and dual variables can be updated in alternating manner. Dual variable updates can be easily done by applying gradient

ascent steps [15] as given in Algorithm 1. Therefore, for the sake of convenience we will derive just primal updates. The updates of Z_1 can be done via

$$Z_1^{k+1} = \arg\min_{Z_1}\{\lambda_2 \|Z_1\|_{2,1} + \langle \beta_1, (Z_1 - X)\rangle + \frac{\mu_1}{2}\|X - Z_1\|_F^2\} \quad (9)$$

which is equivalent to

$$Z_1^{k+1} = \arg\min_{Z_1}\left\{\lambda_2 \|Z_1\|_{2,1;L} + \frac{\mu_1}{2}\left\|Z_1 - \left(X^{k+1} - \frac{\beta_1^k}{\mu_1}\right)\right\|_F^2\right\} \quad (10)$$

This is nothing but the proximal operator of windowed $\ell_{2,1}$-norm,

$$Z_1^{k+1} = prox_{(\frac{\lambda_2}{\mu_1})\|\cdot\|_{2,1;L}}\left(X^{k+1} - \frac{\beta_1^k}{\mu_1}\right). \quad (11)$$

For non-overlapping groups, one can derive it as follows

$$(prox_{\gamma\|\cdot\|_{2,1;L}}(Z))^{i,k} = \begin{cases}\left(1 - \frac{\gamma}{\|\underline{Z}^{i,k}\|}\right)\underline{Z}^{i,k} & \text{if } \gamma < \|\underline{Z}^{i,k}\| \\ 0 & \text{else}\end{cases}$$

by using [16] section 6.5.4, where $\underline{M}^{i,k}$ is the k.th group of row i. For over-lapping case, it will be [17]

$$(prox_{\gamma\|\cdot\|_{2,1}}(Z))(j,k) = \begin{cases}\left(1 - \frac{\gamma}{\|\underline{Z}^{i,k}\|}\right)Z(j,k) & \text{if } \gamma < \|\underline{Z}^{i,k}\| \\ 0 & \text{else}\end{cases}$$

where $M(j,k)$ is the k-th element of j-th row. Similarly, the update of Z_2 will be proximal operator of $\ell_{TV,1}$ as follows

$$Z_2^{k+1} = prox_{(\frac{\lambda_3}{\mu_2})\|\cdot\|_{TV,1}}\left(X^{k+1} - \frac{\beta_2^k}{\mu_2}\right). \quad (12)$$

On can also find the X update equation by solving $\nabla_x L(.) = 0$, because the right hand side of the equation is differentiable. The overall algorithm is given in Algorithm 1, where we define M_d as d-th column of a matrix M.

Algorithm 1 ADMM for Problem

repeat

Primal Updates

$x_d^{k+1} \leftarrow (\lambda_1 F_d^T F_d + I\mu_1 + I\mu_2)^{-1}$
$(\lambda_1 F_d^T y_d + \mu_1 Z_{1_d} + \mu_2 Z_{2_d} + \beta_{1_d}^k + \beta_{2_d}^k)$

$Z_1^{k+1} \leftarrow prox_{(\frac{\lambda_2}{\mu_1})\|\cdot\|_{2,1;L}}\left(X^{k+1} - \frac{\beta_1^k}{\mu_1}\right)$

$Z_2^{k+1} \leftarrow prox_{(\frac{\lambda_3}{\mu_2})\|\cdot\|_{TV,1}}\left(X^{k+1} - \frac{\beta_2^k}{\mu_2}\right)$

Dual Updates:

$\beta_1^{k+1} \leftarrow \beta_1^k + \mu_1(Z_1^{k+1} - X^{k+1})$
$\beta_2^{k+1} \leftarrow \beta_2^k + \mu_2(Z_2^{k+1} - X^{k+1})$

until Convergence

return $\hat{X}$

V. Experiments

A. Experimental setup

In this study, the stepped frequency scanning was performed using the Anritsu vector network analyzer and two horn antennas in the spectral frequency band from 100 MHz to 15 GHz in 201 frequency steps. The receiver and transmitter antenna pairs were shifted 150 times to combine the B-scan data with 2 cm step length along a 3 m fixed x-axis. In the designed scenario, we aimed to detect a target concealed behind the wall. In accordance with this purpose, a metal body model was placed behind a wall of approximately 30 cm to perform the screening. The distance between the antenna pairs and the metal target is 85 cm. Dimensions of the metal body model detailed in the figure are in the rough 44x95 cm.

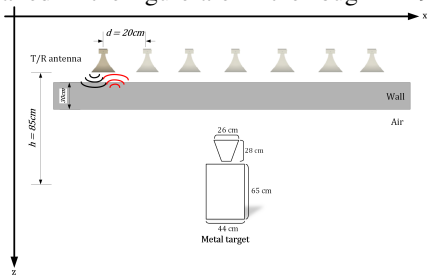

Fig. 8: Measurement scenario concerning with detection of the target behind the wall.

B. Experimental Results

In Figure 4 (a), we shows the B-Scan obtained using from IFFT of all $N = 201$ frequencies. A wall closed the reader and an object in the middle easily identifiable. Figure 4 (b) shows IFFT results of $m = 0.2 * N$ randomly chosen frequencies, we can call it ℓ_2 minimization result. Figure 5 (a) shows the when we randomly choose $m = 0.2 * N$ random frequencies and ℓ_1 minimization method where each A-Scan estimate is done independently. As it is shown in Figure 5 (a) and Figure 6 (a), in ℓ_1 results, object is not identifiable when $m = 0.2$ but when we increase it to $m = 0.4$ it becomes more visible. Both Figure 5-6 (b) shows us then proposed approach when successive A-Scan estimates support each other, object is visible even for $m = 0.2 * N$.

We also extend this experiment to the situation where we exactly know the wall location, despite an improvement in the result of ℓ_1 minimization method due to increase in sparsity level we achieve much more improvement in the result of the proposed method if we consider the location and shape estimate of the object. We use over-lapping groups in that experiment with $L = 10$. As shown in Figure 8, the object length $D = 22$ (22) cm in our experimental setup which is approximately estimated in all experiments.

VI. Conclusion

In this work, we define a random frequency through the all imaging system. Then, we have proposed a new CS reconstruction algorithm working on sliding window mode for this system. This reconstruction method enjoys the information that successive A-Scan signals have similar structures. The algorithm can also be applied in an on-line manner during the measurement process, therefore can help to adaptively

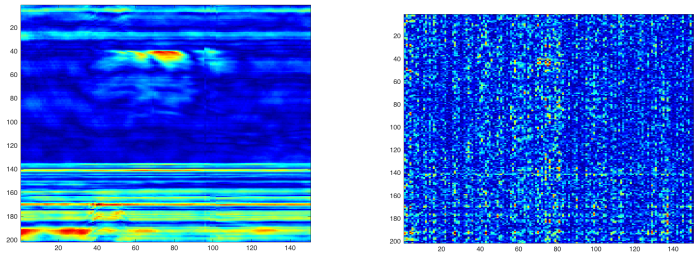

Fig. 4: Estimated B-Scan images. There is a wall through all A-scan and object to be detected in the middle. (a) Non-CS B-scan. IFFT is applied to get A-scan data to $N = 201$ uniformly sampled frequency in the signal band between 0.1 GHz-15GHz. (b) B-scan estimation when IFFT applied to $m = 0.2 * N$ randomly chosen subset of these frequencies.

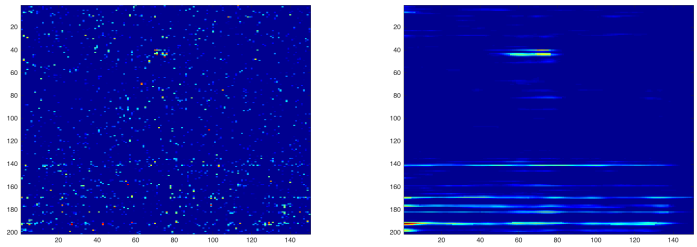

Fig. 5: (a) B-scan estimation when ℓ_1 minimization is applied to randomly chosen $m = 0.2 * N$ frequencies. (b) B-scan estimation of proposed Reconstruction.

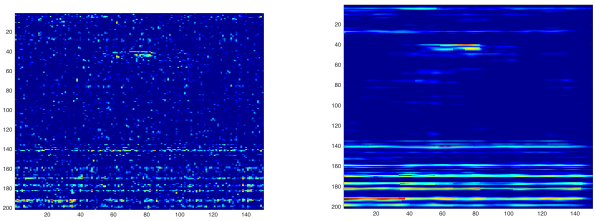

Fig. 6: (a) B-scan estimation when ℓ_1 minimization is applied to randomly chosen $m = 0.4 * N$ frequencies. (b) B-scan estimation of proposed Reconstruction.

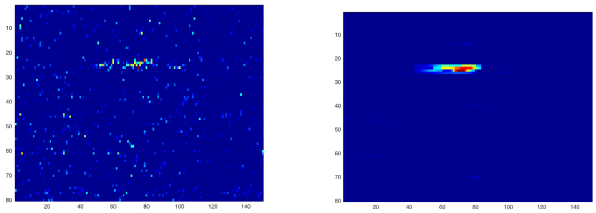

Fig. 7: Estimated B-Scan images when the wall location is known in advance. (a) B-scan estimation when ℓ_1 minimization is applied to randomly chosen $m = 0.2 * N$ frequencies. (b) B-scan estimation of proposed Reconstruction.

change the number of measurements taken in a fixed position. This study can also be extended to the randomized position choosing such as in SAR imaging or randomized B-Scan choosing in C-Scan case.

REFERENCES

[1] Noon, David Andrew. "Stepped-frequency radar design and signal processing enhances ground penetrating radar performance." (1996).

[2] Sugak, Vladimir G., and Alexander V. Sugak. "Phase spectrum of signals in ground-penetrating radar applications." IEEE Transactions on Geoscience and Remote Sensing 48.4 (2010): 1760-1767.

[3] Nguyen, Cam, and Joongsuk Park. Stepped-Frequency Radar Sensors: Theory, Analysis and Design. Springer International Publishing, 2016.

[4] van Genderen, Piet. "Multi-waveform SFCW radar." Microwave Conference, 2003 33rd European. IEEE, 2003.

[5] Suksmono, Andriyan Bayu, et al. "Compressive stepped-frequency continuous-wave ground-penetrating radar." IEEE geoscience and remote sensing letters 7.4 (2010): 665-669.

[6] Yoon, Yeo-Sun, and Moeness G. Amin. "Imaging of behind the wall targets using wideband beamforming with compressive sensing." Statistical Signal Processing, 2009. SSP'09. IEEE/SP 15th Workshop on. IEEE, 2009.

[7] Huang, Qiong, et al. "UWB through-wall imaging based on compressive sensing." IEEE Transactions on Geoscience and Remote Sensing 48.3 (2010): 1408-1415.

[8] Leigsnering, Michael, et al. "Compressive sensing based specular multipath exploitation for through-the-wall radar imaging." Acoustics, Speech and Signal Processing (ICASSP), 2013 IEEE International Conference on. IEEE, 2013.

[9] Gurbuz, Ali Cafer, James H. McClellan, and Waymond R. Scott. "A compressive sensing data acquisition and imaging method for stepped frequency GPRs." IEEE Transactions on Signal Processing 57.7 (2009): 2640-2650.

[10] Yang, Jungang, et al. "Random-frequency SAR imaging based on compressed sensing." IEEE Transactions on Geoscience and Remote Sensing 51.2 (2013): 983-994.

[11] Baraniuk, Richard, and Philippe Steeghs. "Compressive radar imaging." Radar Conference, 2007 IEEE. IEEE, 2007.

[12] Candes, Emmanuel J. "Compressive sampling." Proceedings of the international congress of mathematicians. Vol. 3. 2006.

[13] Candes, E. and J. Romberg, Sparsity and Incoherence in Compressive Sampling, Inverse Problems, Vol. 23, No. 3, p. 969, 2007

[14] Yang, Jungang, et al. "Random-frequency SAR imaging based on compressed sensing." IEEE Transactions on Geoscience and Remote Sensing 51.2 (2013): 983-994.

[15] Boyd, Stephen, et al. "Distributed optimization and statistical learning via the alternating direction method of multipliers." Foundations and Trends in Machine Learning 3.1 (2011): 1-122.

[16] Parikh, Neal, and Stephen P. Boyd. "Proximal Algorithms." Foundations and Trends in optimization 1.3

[17] Kowalski, Matthieu, Kai Siedenburg, and Monika Drfler. "Social sparsity! neighborhood systems enrich structured shrinkage operators." IEEE transactions on signal processing 61.10 (2013): 2498-2511.